Disrupted functional connectivity of precuneus subregions in obsessive-compulsive disorder

Qianqian Ye [a], Zongfeng Zhang [b,c], Wanqing Sun [a], Qing Fan [b,c,*], Yao Li [a,*]

[a] School of Biomedical Engineering, Shanghai Jiao Tong University, Shanghai 200030, PR China
[b] Shanghai Mental Health Center, Shanghai Jiao Tong University School of Medicine, Shanghai 200030, PR China
[c] Shanghai Key Laboratory of Psychotic Disorders, Shanghai, 200030, PR China

ABSTRACT

Obsessive-compulsive disorder (OCD) is a chronic and disabling psychiatric disorder with high lifetime prevalence, yet the underlying pathogenesis remains not fully understood. Increasing neuroimaging evidence has shown that the disrupted activity of brain functional hubs might contribute to the pathophysiology of OCD. Precuneus is an important brain hub which showed structural and functional abnormalities in OCD patients. However, the functional heterogeneity of the precuneus subregion has not been considered and its relation to OCD symptomatology remains to be elucidated. In this paper, a total of 73 unmedicated OCD patients and 79 matched healthy subjects were recruited and the heterogeneous functional connectivities (FCs) of the precuneus subregions were investigated using resting-state functional magnetic resonance imaging. The FC-based subdivision of the precuneus was performed using the K-means clustering algorithm, which led to a tripartite functional parcellation of precuneus. For each subregion, the distinct connectivity pattern with the whole brain was shown, using both voxel-wise and module-wise analysis, respectively. Decreased FC between dorsal posterior precuneus and vermis (corrected $p < 0.01$) was shown in the patient group, which was negatively correlated with patient compulsions score ($\rho = -0.393$, p = 0.001), indicating its contribution to the compulsive behavior inhibition of OCD. Our work might provide new insights into the understanding of precuneus subregion function and the importance of dorsal precuneus-cerebellum functional connectivity in OCD pathophysiology.

1. Introduction

Obsessive-compulsive disorder (OCD) is characterized by intrusive thoughts and repetitive behaviors (Robbins et al., 2019). Despite its high prevalence, the pathogenesis of OCD remains not fully understood. Increasing number of neuroimaging studies suggest that the disrupted activity of brain functional hub is related to the pathophysiology of OCD (Tian et al., 2016; van den Heuvel and Sporns, 2011; Yun et al., 2020). Precuneus is an important brain functional hub in the default mode network (DMN) for the integration of internally and externally driven information (De Domenico et al., 2016; Hwang et al., 2013; van den Heuvel and Sporns, 2011). The structural abnormality of precuneus has been reported in OCD patients, including reduced grey matter volume and increased cortical thickness and white matter volume (Chen et al., 2013; Fan et al., 2012; Park and Jeong, 2015; Rus et al., 2017; Shaw et al., 2015; Tang et al., 2015). Moreover, in task-based functional MRI

studies, the OCD patients showed hyperactivation of precuneus during higher-order cognitive tasks such as working memory, non-affective and obsessive–compulsive symptom provoking tasks (de Vries et al., 2014; Rasgon et al., 2017; Viard et al., 2005; Viol et al., 2019). The increased functional activation of precuneus under neutral emotional stimulation was correlated with patient obsessive and compulsive symptom severity (Thorsen et al., 2018).

Compared to the structural or functional activation studies in OCD, the studies investigating the alteration of intrinsic functional connectivity (FC) of precuneus were rather fewer. Zhang et al. investigated the intrinsic functional connectivity in OCD patients using resting-state functional MRI (rs-fMRI) and found increased FCs in precuneus and cerebellum (Zhang et al., 2011). The significance of cerebellar functional networks has been recognized for long in previous studies (Buckner et al., 2011; Stoodley and Schmahmann, 2009). The subregions within the cerebellum have been shown functionally

connected to distinct cerebral areas, forming complex cerebellar networks (Bostan et al., 2013; O'Reilly et al., 2010). Increasing evidence has shown that the cerebellar networks were closely involved in cognitive process in psychiatric disorders (Hoppenbrouwers et al., 2008; Miquel et al., 2019). Recently, abnormal cerebral-cerebellar functional connectivities have been continuously shown in OCD studies, which provided significant insights into the role of cerebellar networks in OCD pathophysiology (Liu et al., 2020; Moody et al., 2017; Xu et al., 2019).

Because of the non-uniform nature of precuneus cytoarchitecture (von Economo and Koskinas, 1925), its functional heterogeneity has long been recognized (Cavanna and Trimble, 2006; von Economo and Koskinas, 1925; Zhang and Li, 2012). In task-related neuroimaging studies, distinct activities of precuneus subregions were associated with different cognitive functions (Pfefferbaum et al., 2011). Using rs-fMRI, the precuneus subregions also showed very different FC patterns in healthy individuals (Cauda et al., 2010; Margulies et al., 2009; Zhang and Li, 2012). Nevertheless, the functional heterogeneity of precuneus in contribution to OCD pathophysiology has not been explored. We speculate that the high functional heterogeneity of precuneus reduced the sensitivity of detecting the alteration in FC when using the whole precuneus as the seed. The hypothesis of this study is that sub-precuneus functional segmentation could provide useful insights into the heterogeneous FC alterations of precuneus subregions and understanding its role in OCD pathophysiology. Moreover, beyond the cerebral networks, the sub-precuneus to cerebellar functional connectivity might shed light on the symptomology of OCD patients.

To validate our hypothesis, seventy-three unmedicated OCD patients with seventy-nine matched healthy subjects were included in the work. The FC-based subdivision of the precuneus was performed using K-means clustering algorithm. The FCs of each precuneus subregion to the rest of the brain were measured and compared between heathy controls and OCD patients at both module-level and voxel-level, respectively. The aim is to understand the distinct FC alterations of each functional subregion of precuneus in OCD to provide useful insights into its pathophysiology.

2. Methods and materials

2.1. Participants

All the participants were recruited from Shanghai Mental Health Center, including 73 unmedicated OCD patients (mean age: 28.93 ± 5.33, range: 18–45 years) and 79 healthy controls (HCs) (mean age: 27.73 ± 5.71, range: 20–47 years) matched with age, gender, and education level (Table 1). We used the Yale-Brown Obsessive-Compulsive Scale (Y-BOCS) to assess OCD symptom severity (Goodman et al., 1989). All patients met DSM-IV diagnostic criteria for OCD (American Psychiatric Association, 2003), without psychotropic medication for at least 8 weeks. Exclusion criteria for all the subjects included neurological

Table 1
Demographic information of OCD patients and healthy controls.

Characteristics	OCD (n = 73)	HC (n = 79)	p value
Age (years)	28.93 ± 5.33	27.73 ± 5.71	0.183[a]
Gender: Male/Female	38/35	42/37	0.490[b]
Education (years)	15.05 ± 2.07	15.62 ± 2.17	0.102[a]
Duration (years)	8.81 ± 5.97	/	/
Age of onset (years)	20.11 ± 6.51		
YBOCS-obsessions	14.04 ± 3.02	/	/
YBOCS-compulsions	11.51 ± 4.00	/	/
YBOCS-total	25.55 ± 5.73	/	/

Note: Data are presented as mean ± SD.
Abbreviations:HC, healthy controls; OCD, obsessive–compulsive disorder; YBOCS, Yale-Brown Obsessive-Compulsive Scale.
[a] Independent two-sample *t*-test.
[b] Chi-square test.

disorder, head injury or physical disease, history of drug or alcohol addiction, pregnancy, and cardiac pacemaker or other metallic implants. The study was approved by the Institutional Review Board of Shanghai Mental Health Center. Written informed consent was obtained from each participant.

2.2. Image acquisition

All the imaging data were acquired on a 3 T Siemens Verio MR scanner. During the scan, the participants were instructed to lay supine with eyes closed but remain awake and avoid systematic thinking. Structural images were acquired with a T1-weighted magnetization prepared rapid gradient echo (MPRAGE) sequence. The imaging parameters are as follows: repetition time (TR) = 2300 ms, echo time (TE) = 2.96 ms; flip angle (FA) = 9°; inversion time (TI) = 900 ms; acquisition matrix = 256 × 256; slice number = 192; thickness = 1 mm; voxel size = $1.0 \times 1.0 \times 1.0$ mm^3. The resting-state fMRI data were acquired using a gradient-echo Echo Planar Imaging (EPI) sequence with the following parameters: acquisition matrix = 64 × 64; field of view (FOV) = 220 mm; TR/TE/FA = 2000 ms/30 ms/90°; band width = 2298 Hz/pixel; slice number = 30; slice thickness = 4 mm; gap = 0.5 mm; voxel size = $3.4 \times 3.4 \times 4.0$ mm^3, and total volume number = 180.

2.3. fMRI data preprocessing

The fMRI data were preprocessed using the Analysis of Functional Neuroimaging (AFNI) software package (Cox, 1996). The first four volumes were removed to allow the subject's adaptation to scanning noise and signal equilibrium and reserve as much useful information, following the previous literature (Kellermann et al., 2013; Liang et al., 2013). The remaining 176 fMRI images were realigned to the first volume for correction of acquisition time delay after spikes removal. The images were spatially normalized to the space of the Montreal Neurological Institute (MNI) 152 template with a resampled resolution of 3 × 3 × 3 mm^3. Temporal band-pass filtering (0.01–0.1 Hz) was performed to reduce the effect of low-frequency drifts and high-frequency physiological noises. The nuisance signals, including 6 realignment parameters and their first derivatives, averaged signals from white matter (WM), cerebral spinal fluid (CSF) and whole brain, were regressed out from the data. Finally, spatial smoothing was applied for all images with a 6 mm full width at half maximum (FWHM) Gaussian kernel. To minimize the head motion effect, we excluded the participants with more than 0.25 mm mean framewise displacement (FD) and censored the data points with FD over 0.3 mm (Power et al., 2012).

2.4. Precuneus functional parcellation

The functional parcellation of precuneus was based on the whole-brain FCs using a K-means clustering algorithm (Kahnt et al., 2012; Kahnt and Tobler, 2017). For each voxel within the precuneus region of an individual subject, as defined by the anatomical automatic label (AAL) template (https://www.gin.cnrs.fr/en/tools/aal/, AAL1), we calculated its connectivities with all other voxels in the gray matter mask by Pearson correlation analyses (Tzourio-Mazoyer et al., 2002). The correlation coefficient matrices after Fisher's Z-transformation were averaged across subjects to get the group average whole-brain connectivity for each voxel of precuneus. The resulting connectivity vectors (one per precuneus voxel) were then used to group together the precuneus voxels that have a similar connectivity profile with the rest of the brain. The functional parcellation was carried out using the K-means clustering algorithm (Tou and González, 1974). The parcellation was optimized by minimizing the squared error function:

$$J = \sum_{j=1}^{K} \sum_{i=1}^{n} \left\| v_i^{(j)} - c_j \right\|^2$$

where $v_i^{(j)}$ is voxel i in cluster j, c_j is the centroid of cluster j, n is the total number of voxels, $\|v_i^{(j)} - c_j\|$ represents a distance measure between $v_i^{(j)}$ and c_j. Given this, the voxels that show similar connectivity profiles with the rest of the brain tend to be clustered together. The algorithm was implemented in MATLAB.

To determine the optimal cluster number K, we compared the cluster compactness for each K ranged from 2 to 4 (Ray and Turi, 1999). The cluster compactness (CP) is defined as the ratio of D_{inter}/D_{intra}, where D_{inter} and D_{intra} denote the distances within and between clusters, respectively:

$$D_{inter} = mean(\|z_i - z_j\|^2), i = 1, 2, \cdots, K-1, j = i+1, i+2, \cdots, K,$$

$$D_{intra} = \frac{1}{N} \sum_{i=1}^{K} \sum_{x \in C_i} \|x - z_i\|^2$$

where N is the number of voxels, z_i and z_j are the centers of their corresponding clusters C_i and C_j, respectively. The optimal K value was to minimize the within-cluster distance and maximize the between-cluster distance, thus leading to a maximum CP. The metric that was applied in our study for the optimal selection of the subregion number is a bit empirical, which was based on the previous literature that suggested the division of precuneus into three subregions, in agreement with its tripartite cytoarchitecture. Wang et al. used both anatomical connectivity and task-dependent coactivation patterns to parcellate the human precuneus and consistently found three subregions in it (Wang et al., 2019). Zhang et al. utilized Bayesian Information Criterion (BIC) to determine the optimal number of clusters for their K-means parcellation of precuneus. And they found that the identified eight clusters could be broadly divided into dorsal-anterior, dorsal-posterior, and ventral parts. Thus these three subregions were used for their further FC analysis(Luo et al., 2020). Given this, we restricted our comparison set to K = 2 to 4. The mean time series of each parcelled precuneus subregion was used for correlation analysis with the rest of the brain to obtain the corresponding FC maps.

2.5. Functional modular analysis

To investigate the connectivity of precuneus with different brain networks, we performed a whole brain functional parcellation based on resting-state functional connectivity (RSFC). First, the time course of each voxel within the group-averaged grey matter mask was extracted and the Pearson's correlations were performed to create a whole brain connectivity matrix. The obtained connectivity matrix was transformed into Fisher's z-map for normalization. To eliminate the effects from global signal and noise, a binary connectivity matrix was created with the data assigned to 1 if greater than 0r.2 and 0 otherwise (Dai et al., 2015). By averaging the subject-specific binary matrix and discarding the connections present in less than half of the group subjects, we obtained the group mean FC matrix. For module identification, we used a random-walk-based infomap algorithm because of its advantages in handling large networks and stability in complex conditions (Puxeddu et al., 2017; Rosvall and Bergstrom, 2008). The determination of optimal modular structure was performed based on the modularity parameter Q defined as (Newman and Girvan, 2004):

$$Q = \frac{1}{L} \sum_{i,j \in N} [w_{ij} - \frac{k_i k_j}{L}] \delta_{m_i, m_j}$$

where i, j represent two individual nodes, L is the sum of all edges in the network, w_{ij} the connectivity strength between nodes i and j, k_i the sum of edges linked to node i, m_i the module where node i belongs to. A network with a strong modular structure typically has a modularity Q ranged from 0.3 to 0.7 (Newman and Girvan, 2004). Individual mean time-course within each module of interest was extracted for further FC

analysis.

2.6. Statistical analysis

All the statistical analyses were performed using SPSS software (SPSS Inc, Chicago, III, USA, version 19.0). The one-sample t-tests were used to analyze the FC changes of precuneus subregions in each group. The FC maps were compared between patient and control groups using two-tailed two-sample t-tests implemented in a MATLAB-based Resting-State FMRI Data Analysis Toolkit (REST1.8, http://www.restfmri.net). The statistical threshold was set as $p_{corrected} < 0.05$ using Alphasim correction (voxel threshold $p < 0.005$, minimum cluster size = 702 mm^3, FWHM = 6 mm, number of iterations = 1000). The correlations between precuneus functional connectivity and clinical symptom measures were calculated using Spearman correlation analysis. The Bonferroni corrections were applied for multiple comparisons for both module-wise and voxel-wise correlation analyses.

3. Results

#### 3.1. Demographic characteristics and clinical variables

In our cohort, no significant differences were found in demographic variables including age, gender, and educational status between OCD patients and healthy controls, as shown in Table 1. The mean Yale--Brown Obsessive Compulsive Scale (YBOCS) total score for OCD patients is 25.55 (SD = 5.73), corresponding to a moderate symptom severity, with mean obsessions score equal to 11.51 (SD = 4) and mean compulsions score equal to 14.04 (SD = 3.02). The mean duration of illness of patients is 8.81 years (SD = 5.97), and the mean age of onset is 20.11 (SD = 6.51).

3.2. Different functional connectivity patterns of precuneus subregions

The optimal parcellation of precuneus was determined based on the cluster compactness value. The parcellation results along with the correlation matrices for K = 2 to 4 were illustrated in Fig. 1. Each data in the matrices represents the voxel-wise correlation of the connectivity profile with the rest of the brain for each precuneus voxel. The robustness of the parcellation performance was further shown using OCD group, HC group, as well as both groups, respectively (Supplementary Fig. 1). We used the parcellation results derived from using both healthy control and OCD patient data to incorporate the precuneus functional variations of both groups. The optimal cluster number was determined as K = 3, which achieved the highest compactness value (11.2±4.3). Therefore, the precuneus was divided into dorsal anterior (DA-pcu), dorsal posterior (DP-pcu) and ventral (V-pcu) subregions.

Using functional modular analysis, we identified five cerebral functional modules: the central executive network (CEN), default mode network (DMN), sensorimotor network (SM), salience network (SN), and visual network (VN). Moreover, five cerebellar networks were also extracted, including anterior lobe (AL), inferior posterior lobe (IPL), middle posterior lobe (MPL), superior posterior lobe (SPL), and vermis posterior lobe (VPL) (Fig. 2A). The modular parcellation results were confirmed using group-averaged networks of the OCD and HC groups, respectively, as illustrated in Supplementary Fig. 2. As can been seen, the identified modules in our analysis were consistent across both groups.

Each subregion of precuneus showed different FC pattern with the brain functional modules (Fig. 2B-D). The DA-pcu exhibited positive FCs with SM, SN, IPL and VPL, as well as negative FCs with CEN, DMN, SPL and AL ($p < 0.001$). The DP-pcu showed positive FCs with VN, IPL and VPL, as well as negative FCs with SN and SM ($p < 0.001$). The V-pcu was positively correlated with DMN and SPL, and negatively correlated with CEN, SM, SN, IPL and MPL ($p < 0.001$). These results suggested that each subregion had different functional connectivity patterns to
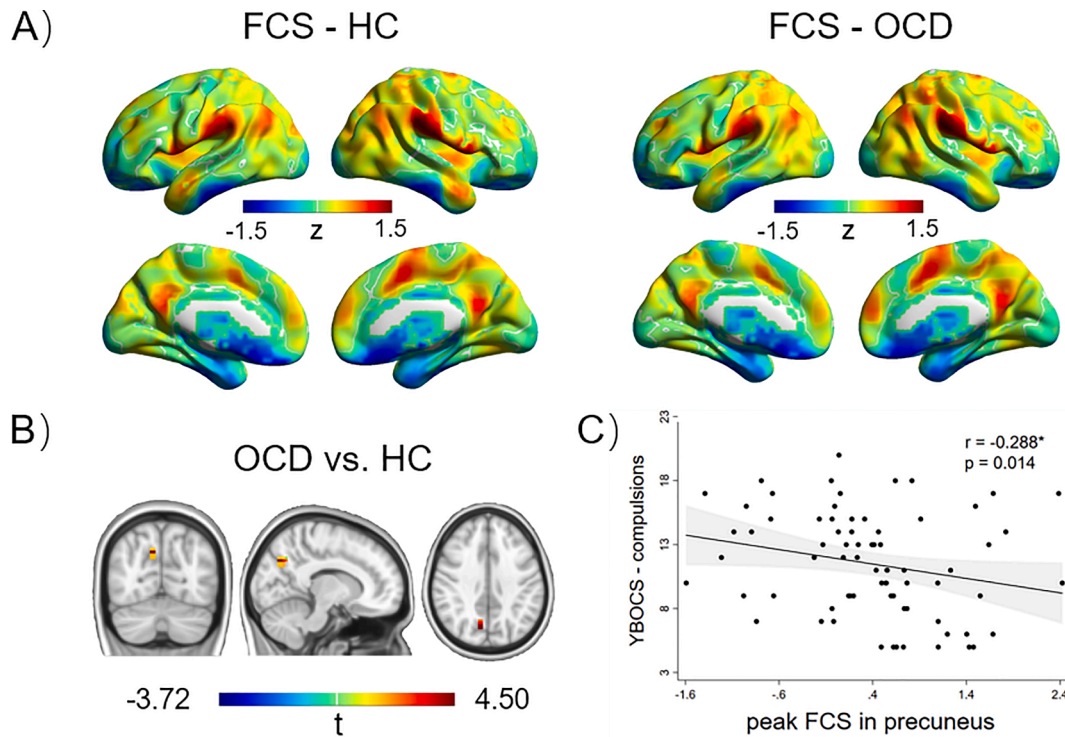
Fig. 1. Functional parcellation of precuneus using K-means clustering method based on the whole brain voxel-wise functional connectivity for (A) K = 2, (B) K = 3, and (C) K = 4, respectively. Top: the corresponding correlation matrix. Bottom: the parcellation results with the associated compactness values (CPs).
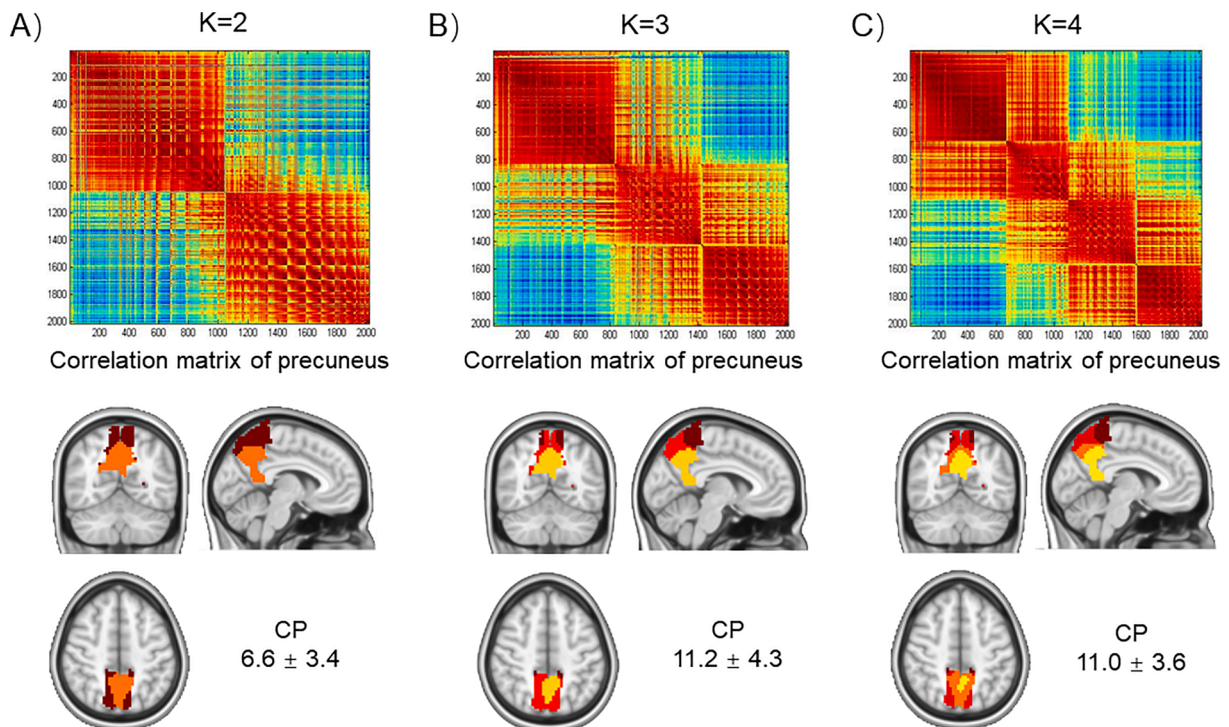
Fig. 2. Module-wise analysis of the functional connectivity patterns of precuneus subregions. (A) Functional modular parcellation of the whole brain, including five cerebral networks and five cerebellar networks. (B) Functional connectivity between DA-pcu and different brain networks. C) Functional connectivity between DP-pcu and different brain networks. D) Functional connectivity between V-pcu and different brain networks. Abbreviations: AL, anterior lobe; CC, cerebral cortex; CE, cerebellum; CEN, central executive network; DA-pcu, dorsal anterior precuneus; DMN, default mode network; IPL, inferior posterior lobe; MPL, middle posterior lobe; SPL, superior posterior lobe; SM, sensorimotor network; SN, salience network; V-pcu, ventral precuneus; VN, visual network; VPL, vermis posterior lobe.

different functional modules, which confirmed the functional heterogeneity of precuneus. Morevoer, the FCs between each functional subregion of precuneus and the ten functional networks parcellated were compared between HC and OCD groups. The FC between V-PCu and MPL module showed a trend toward significance for the between-group FC difference (p = 0.066), as shown in Supplementary Table 1.

3.3. Disrupted whole brain functional connectivity of precuneus subregions in OCD patients

The whole brain functional connectivity maps for each precuneus subregion showed similar connectivity patterns between OCD and HC groups (Fig. 3A). In general, the DA-pcu connected more closely with mid-frontal lobe and motor cortex, while the DP-pcu showed higher connectivity with superior frontal cortex and visual cortex. The V-pcu showed higher FCs with medial frontal lobes, post cingulate cortex and angular gyrus, as well as lower FCs with inferior frontal lobes and insula. The between-group FC map comparisons for each precuneus subregion are shown in Fig. 3B.

In the group of OCD patients, the DA-pcu showed a decreased FC with the right lingual gyrus, while both DA-pcu and DP-pcu had increased FCs with the left parietal cortex. Besides, the DP-pcu had a decreased FC with left cerebellum in OCD patients compared with HC groups, specifically with the Crus I and vermis regions. OCD patients showed decreased FCs between V-pcu and left superior frontal gyrus, as well as the cerebellum posterior lobe. The altered precuneus subregion FCs in OCD patients were listed in Table 2.
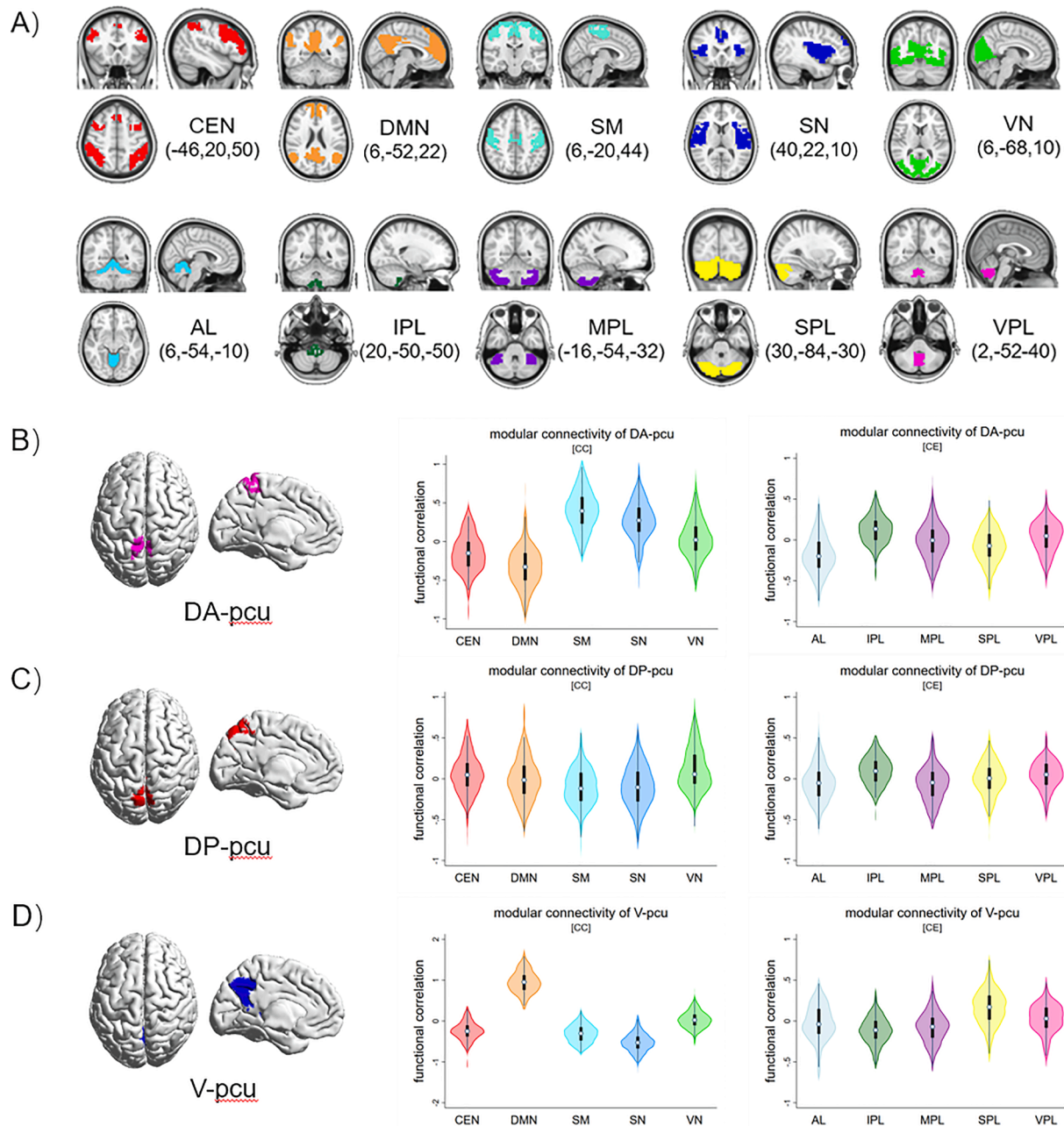
Fig. 3. Voxel-wise analysis of the functional connectivity patterns of precuneus subregions. (A) Functional connectivity maps of DA-pcu, DP-pcu and V-pcu in OCD and HC group, respectively. (B) Between-group comparisons of whole-brain voxel-wise functional connectivity from DA-pcu, DP-pcu and V-pcu, respectively. Abbreviations: HC, healthy controls; OCD, obsessive–compulsive disorder; DA-pcu, dorsal anterior precuneus; DP-pcu, dorsal posterior precuneus; V-pcu, ventral precuneus.

Table 2
Brain regions showing significant functional connectivity differences of the precuneus subregions between OCD patients and healthy controls.

| No.	Peak MNI coordinate			Peak t	Brain region (L: left, R: right)	p$_{corrected}$
	x	y	z			
Seed: dorsal-anterior precuneus (DA-pcu)						
1	6	−69	−3	−4.1143	R_lingual gyrus	<0.001
2	−60	−30	51	4.1195	L_parietal cortex	<0.001
Seed: dorsal-posterior precuneus (DP-pcu)						
1	−9	−81	−21	−3.7826	L_cerebellum Crus I	<0.001
2	−3	−66	−6	−3.3694	L_cerebellum vermis	0.008
3	−51	−36	57	3.9514	L_parietal cortex	<0.001
Seed: ventral precuneus (V-pcu)						
1	45	−60	−51	−4.4561	R_cerebellum	0.006
2	−21	63	3	−3.7207	L_superior frontal cortex	0.006

3.4. Correlations between precuneus subregional functional connectivity and symptomology of OCD patients

For the voxel-wise correlation analysis, the reduced DP-pcu to vermis connectivity was associated with OCD patients YBOCS-compulsions score ($\rho = -0.393$, p = 0.001) and total score ($\rho = -0.393$, p = 0.001) (Fig. 4). For the module-wise correlation analysis, the FC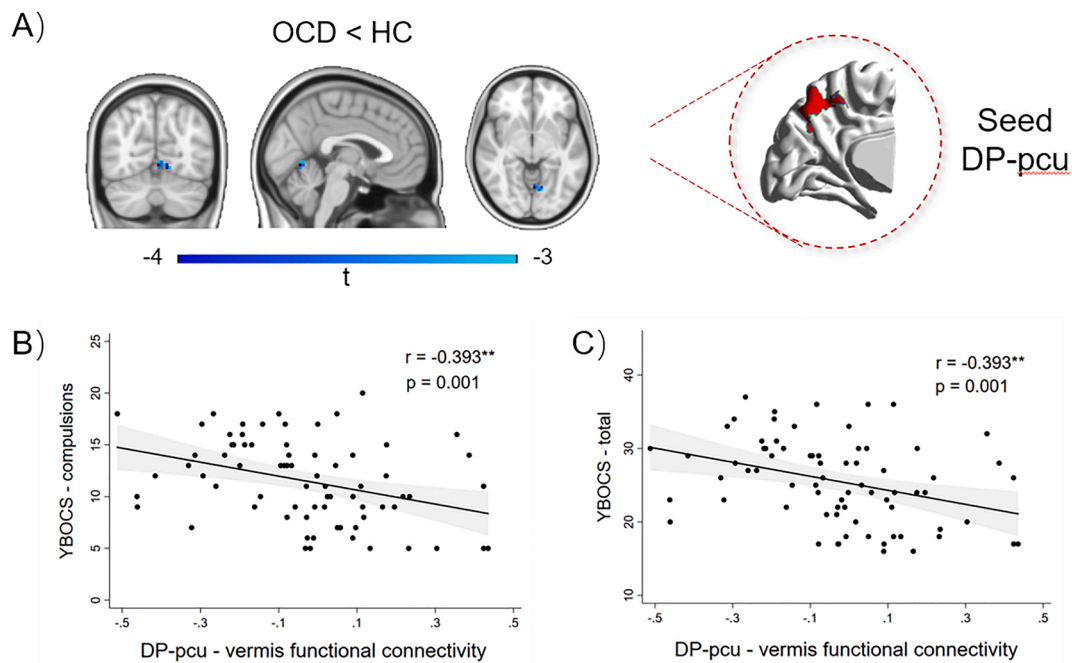 between DP-pcu and cerebellar AL was negatively correlated with patients YBOCS-total score ($\rho = -0.358$, p = 0.002) (Fig. 5A). The functional connectivity between V-pcu and cerebellar AL was negatively correlated with patients YBOCS-total score ($\rho = -0.393$, p = 0.001) (Fig. 5B). The reduced DA-pcu and VN connectivity was negatively associated with patients YBOCS-total score ($\rho = -0.380$, p = 0.001) (Fig. 5C).

3.5. The functional connectivity features of whole precuneus

To show the superiority of performing subregional parcellation of precuneus, we re-examined the FC of using the whole precuneus as the seed and its relation to OCD symptomatology. First, the whole-brain FC maps using the whole precuneus as the seed were obtained for both HC and OCD groups, as shown in Supplementary Fig. 3. No between-group differences were found using two-sample t tests, which might be due to the low sensitivity of the signal. Furthermore, the whole precuneus and AL module (PCu-AL) FC was calculated and its correlation with OCD patient YBOCS total score was evaluated, which was shown in Supplementary Fig. 4. As can be seen, the PCu-AL FC and YBOCS total score had a much weaker correlation, which could not survive the multiple comparison correction ($\rho = -0.241$, p = 0.040). In comparison with that,
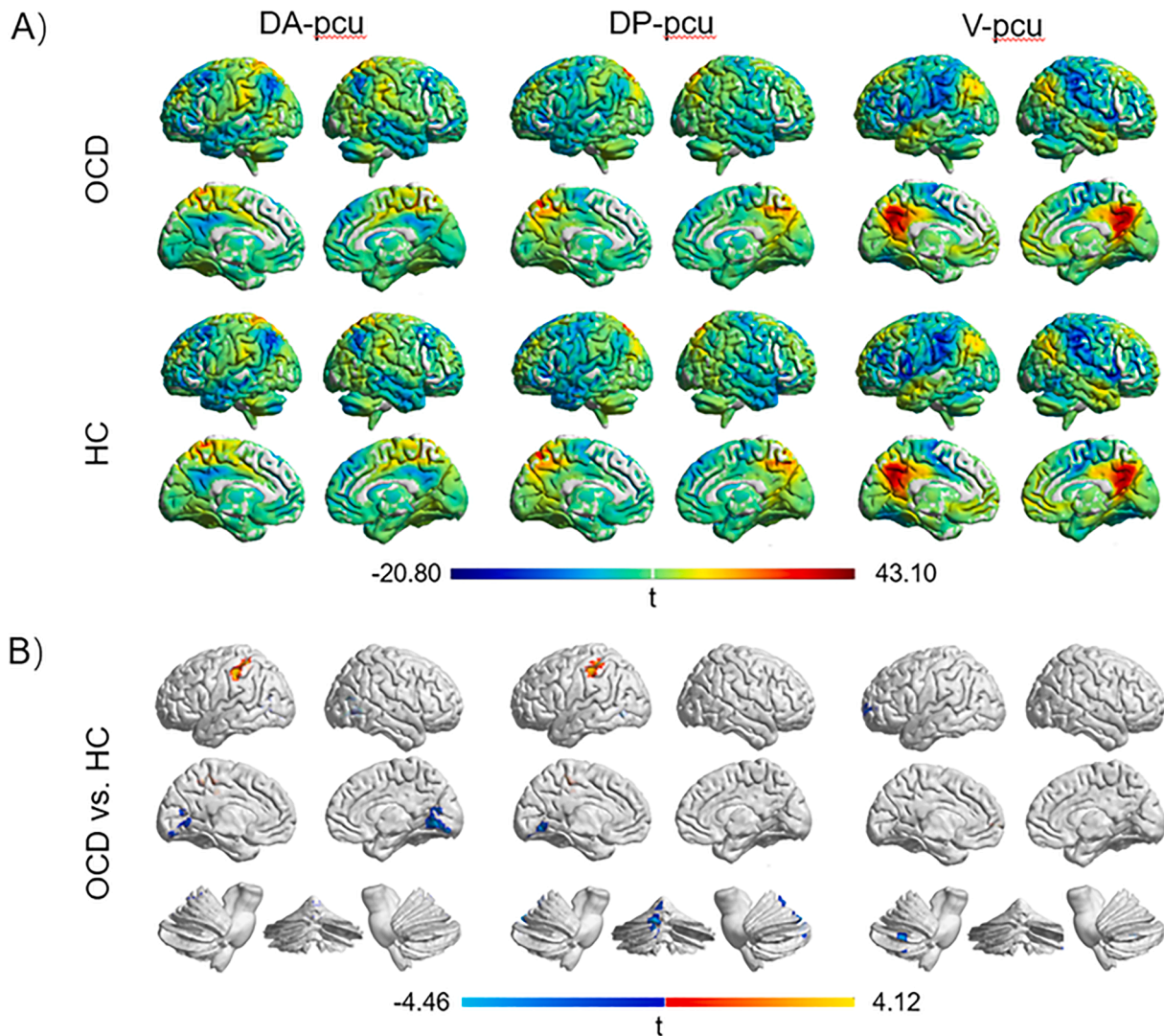
Fig. 4. Correlations between the decreased DP-pcu to vermis FC and clinical scores of OCD patients. (A) OCD patients showed significantly decreased FC between DP-pcu and vermis. (B) The decreased FCs were negatively correlated with patients YBOCS-compulsions scores, and (C) YBOCS-total scores. Abbreviations: OCD, obsessive–compulsive disorder; FC, functional connectivity; DP-pcu, dorsal posterior precuneus; YBOCS, Yale-Brown Obsessive-Compulsive Scale.

Fig. 5. Correlations between the altered precuneus subregion-to-functional module connectivities with OCD clinical scores. (A) FC between DP-pcu and AL, (B) FC between V-pcu and AL, and (C) FC between DA-pcu and VN were negatively correlated with patients YBOCS-total score, respectively. Abbreviations: FC, functional connectivity; DA-pcu, dorsal anterior precuneus; DP-pcu, dorsal posterior precuneus; V-pcu, ventral precuneus; YBOCS, Yale-Brown Obsessive-Compulsive Scale.

the correlations with YBOCS total score for DP-PCu and V-PCu were much more significant (DP-PCu: $\rho = -0.358$, p = 0.002; V-PCu: $\rho = -0.393$, p = 0.001), both surviving multiple comparisons. These results validated the functional heterogeneity of precuneus and necessity to define the functional subregions of it in OCD study.

4. Discussion

The precuneus serves as an important functional hub of the brain with close connections to both cortical and subcortical regions (Cavanna and Trimble, 2006). In our study, the functional heterogeneity of precuneus and its distinct subregional functional connectivities with the brain were shown, using both voxel-wise and module-wise analyses. The tripartite functional parcellation of precuneus was consistent with the literature from the perspective of its anatomical or functional features (Cavanna and Trimble, 2006; Zilles et al., 2003). Wang et al. achieved similar division of precuneus as ours, which included two dorsal and one ventral subregions, based on both anatomical connectivity and task-dependent coactivation patterns (Wang et al., 2019).

In our study, the DA-pcu showed increased connectivity with parietal lobe, sensorimotor area and visual cortex. Modular analysis also showed higher connectivity between DA-pcu and SM and SN. The relevance of DA-pcu to visual cortex has been shown in previous task-based fMRI studies, e.g., the activation of DA-pcu in spatial attention task (Astafiev et al., 2003; Wenderoth et al., 2005). The role of dorsal precuneus in mediating behavioral engagement has been shown using task-related functional activity analysis (Zhang and Li, 2010, 2012). On the other hand, the DP-pcu showed higher functional connectivity with prefrontal cortex, posterior cingulate cortex and visual network. The co-activation of precuneus and prefrontal regions might represent a prerequisite for task-elicited and state-dependent awareness, through the integration between association process and executive function (Cavanna and Trimble, 2006). Finally, we found that the V-pcu was connected with medial frontal and temporal lobes, as well as DMN. The functional activations of ventral precuneus were related with episodic memory retrieval and self-related processing in task-based fMRI studies. These functions were closely related to DMN functional characteristics, which

might explain our findings (Gilboa et al., 2004; Henson et al., 1999; Ochsner et al., 2004).

Besides the cortical regions, we found different connectivity features of precuneus subregions with cerebellum. The cerebellum is functionally responsible for the coordination of movements and modulation of neurological functions for the patients with cognitive deficits (Josef, 2001; Schmahmann, 1998, 2004). The 'internal model' theory was proposed for the explanation about how the cerebellar system contributes to both motor and cognitive functions (Ramnani, 2006), based on which the neural representations are acquired through experience learning to simulate motor or cognitive function (Allen and Tsukahara, 1974). The input–output relationship between neural commands and their consequences was encoded and continuously refined in the internal model (Ramnani, 2006). The diverse information processing in the cerebellar cortex arises from different cerebral inputs to the cerebellum, leading to its functional heterogeneity. In our study, five cerebellar networks were identified, i.e., SPL, IPL, AL, MPL and VPL. The SPL contains Crus I and Crus II, which send and receive projections from prefrontal cortex and form the closed-loop circuits (Bostan et al., 2013). The IPL was associated with the function of DMN (Christophe et al., 2009; Krienen and Buckner, 2009). The AL and MPL contain the sensorimotor regions in the cerebellum (Buckner et al., 2011; Stoodley and Schmahmann, 2009). The VPL, i.e., posterior vermis, was considered as the "limbic cerebellum" because of its close connections with the limbic structure of the brain (Schmahmann, 2004). In our study, the DP-pcu and DA-pcu showed higher connectivity with IPL and VPL, while V-pcu was correlated with SPL activity. The co-activation of dorsal precuneus and cerebellar vermis has been shown in previous motor task study (Wu et al., 2013), while the ventral precuneus was shown correlated with Crus I intrinsic activity (Krienen and Buckner, 2009). Using the module-level FC analysis, the heterogeneous intrinsic functional coupling between precuneus and cerebellum subregions were revealed in our work.

In our findings, the decreased FC between DP-pcu and anterior lobe vermis was negatively correlated with OCD patient YBOCS-compulsions and total scores, which were consistently shown by both voxel-wise and module-wise analyses. The functional activation of precuneus has been

shown related to OCD patients symptom provocation (Rotge and Guehl, 2008). Hu et al. showed increased regional homogeneity in dorsal posterior precuneus along with decreased regional homogeneity in the anterior lobe of cerebellum in OCD patients (Hu et al., 2019). Our results further indicated the close relationship of this functional connectivity with OCD symptomology. The increased connectivity between dorsal precuneus and Crus I was associated with the improved compulsion symptoms after the cognitive-behavioral therapy for OCD patients (Moody et al., 2017). Moreover, it has been shown that lesions in the posterior cerebellar vermis resulted in a delay in behavioral inhibition (Callu et al., 2007), affective dysregulation, and deficits in executive function (Miquel et al., 2019). Interestingly, in our work, the area that showed reduced connectivity with DP-pcu which was negatively associated with patient compulsions score, is located at the intersection of vermis and Crus I. This finding consolidated the important role of this specific connectivity in disrupted behavioral inhibition in OCD patients. As suggested by the internal model theory of cerebellum, the sensory information is integrated to form a perception in temporo-parietal association area and then transferred to cerebellum (Ito, 2008). We hypothesize that the disrupted precuneus-cerebellum connectivity in OCD patients might lead to a less effective access to the internal model (Ramnani, 2006), which reduced their flexibility in behavioral inhibition control. These results suggest the importance of including cerebellar region in the coverage of scan when designing the imaging protocol for future OCD studies.

There are several limitations in our study. First, as a stricter threshold could reduce the possibility of false negative results, the results might be more accurate if using $p < 0.001$ as the threshold for voxel-level between-group comparisons of the FC maps. The difference in the connectivity between DP-PCu and parietal lobe remained significant using $p < 0.001$, while the finding of decreased connectivity between DP-PCu and vermis in OCD group could not survive such a strict threshold (See Supplementary Fig. 5). Given the moderate sample size of our study, future studies with a larger sample size is in need to consolidate our findings. Second, the segmentation was performed using the precuneus region defined from the AAL template, which might not well match its functional region. The functional boundary of sub-precuneus region may extend beyond the original AAL template. In future work, it might be better to extend the clustering analysis to a larger region around precuneus to capture its functional features. To benchmark the performance of our results, we extended the original precuneus mask defined by AAL template about 6 mm to obtain a broader functional mask. The functional parcellation was performed again on the redefined functional precuneus mask. The comparison between the original and new parcellation results are shown in Supplementary Figure 6(A). As can be seen, the functional parcellation of precuneus was stable for both cases. To show the robustness of the clinical correlations, the DP-pcu and AL FC was re-calculated using the extended-AAL template for the parcellation. As shown in Supplementary Figure 6(B), the FC was still significantly correlated with patient YBOCS-total score. Finally, the determination of cluster number is one of the key questions for k-means clustering method. The metric that was applied in our study for the optimal selection of the subregion number was empirical. To show the robustness of our findings in this study, we also performed the group comparison analyses using $K = 2$ and $K = 4$. The results are shown in Supplementary Figure 7 and Supplementary Figure 8, and Supplementary Table 2 and Supplementary Table 3. As can be seen, the FC changes of the precuneus subregions were consistently found in several key regions reported in our study, including lingual gyrus, parietal cortex, cerebellum posterior lobe, cerebellum anterior lobe and cerebellum vermis. Moreover, the FC alterations between dorsal pcu and cerebellum were consistently correlated with and the clinical symptomatology of OCD patients when using $K = 2$ and $K = 4$. When using $K = 2$, the FC of dorsal pcu-vermis was correlated with patients YBOCS-compulsions score ($\rho = -0.257$, $p = 0.028$) and YBOCS-total score ($\rho = -0.265$, $p = 0.023$). When using $K = 4$, the FC of dorsal and posterior pcu-vermis

was correlated with patients YBOCS-compulsions score (dorsal: $\rho = -0.341$, $p = 0.003$; posterior: $\rho = -0.377$, $p = 0.001$) and YBOCS-total score (dorsal: $\rho = -0.339$, $p = 0.003$; posterior: $\rho = -0.428$, $p < 0.001$). The FC of dorsal pcu-AL when using $K = 2$ was correlated with patients YBOCS-total score ($\rho = -0.338$, $p = 0.003$). The FC of dorsal pcu-AL or posterior pcu -AL when using $K = 4$ was also correlated with patients YBOCS-total score (dorsal: $\rho = -0.345$, $p = 0.003$; posterior: $\rho = -0.245$, $p = 0.037$). These results consolidated our findings that alterations in the FC between dorsal precuneus and cerebellum were closely associated with OCD clinical symptomology and might play an important role in OCD pathophysiology. Recently, Luo et al. showed that an eigen clustering (EIC) approach might provide a more delicate level of precuneus parcellation, which might be explored in future studies (Luo et al., 2019).

5. Conclusion

In conclusion, our study showed the functional heterogeneity of precuneus as well as its altered subregional FC features in OCD patients. The FC between DP-pcu and vermis was negatively correlated with the patient compulsions score, indicating their contributions in compulsive behavior inhibition of OCD. Our work provides insights into the understanding of the precuneus subregional function, especially the dorsal precuneus-cerebellum functional connectivity in OCD pathophysiology.

Declaration of Competing Interest

The authors declare that they have no known competing financial interests or personal relationships that could have appeared to influence the work reported in this paper.

Appendix A. Supplementary data

Supplementary data to this article can be found online at https://doi.org/10.1016/j.nicl.2021.102720.

References:

Allen, G.I., Tsukahara, N., 1974. Cerebrocerebellar communication systems. Physiol. Rev. 54, 957–1006.

American Psychiatric Association, 2003. Diagnostic and Statistical Manual of Mental Disorders: DSM-IV., Vol., APA.

Astafiev, S.V., et al., 2003. Functional organization of human intraparietal and frontal cortex for attending, looking, and pointing. J. Neurosci. 23, 4689–4699.

Bostan, A.C., Dum, R.P., Strick, P.L., 2013. Cerebellar networks with the cerebral cortex and basal ganglia. Trends Cogn Sci. 17, 241–254.

Buckner, R.L., et al., 2011. The organization of the human cerebellum estimated by intrinsic functional connectivity. J. Neurophysiol. 106, 2322–2345.

Callu, D., et al., 2007. Habit learning dissociation in rats with lesions to the vermis and the interpositus of the cerebellum. Neurobiol. Dis. 27, 228–237.

Cauda, F., et al., 2010. Functional connectivity of the posteromedial cortex. PLoS ONE 5.

Cavanna, A.E., Trimble, M.R., 2006. The precuneus: a review of its functional anatomy and behavioural correlates. Brain. 129, 564–583.

Chen, J., et al., 2013. Widespread decreased grey and white matter in paediatric obsessive-compulsive disorder (OCD): a voxel-based morphometric MRI study. Psychiatry Res. 213, 11–17.

Christophe, H., et al., 2009. Distinct cerebellar contributions to intrinsic connectivity networks. J. Neurosci. 47, 8586–8594.

Cox, R.W., 1996. AFNI: software for analysis and visualization of functional magnetic resonance neuroimages. Comput. Biomed. Res. 29, 162.

Dai, Z., et al., 2015. Identifying and mapping connectivity patterns of brain network hubs in Alzheimer's disease. Cereb. Cortex 25, 3723–3742.

De Domenico, M., Sasai, S., Arenas, A., 2016. Mapping multiplex hubs in human functional brain networks. Front. Neurosci. 10, 326.

de Vries, F.E., et al., 2014. Compensatory frontoparietal activity during working memory: an endophenotype of obsessive-compulsive disorder. Biol. Psychiatry 76, 878–887.

Fan, Q., et al., 2012. Surface anatomical profile of the cerebral cortex in obsessive–compulsive disorder: a study of cortical thickness, folding and surface area. Psychol. Med. 43, 1081–1091.

Gilboa, A., et al., 2004. Remembering our past: functional neuroanatomy of recollection of recent and very remote personal events. Cereb. Cortex 14, 1214–1225.

Goodman, W.K., et al., 1989. The Yale-Brown Obsessive Compulsive Scale. I. Development, use, and reliability. Arch. Gen. Psychiatry 46, 1012.

Henson, R.N.A., et al., 1999. Recollection and Familiarity in Recognition Memory: An Event-Related Functional Magnetic Resonance Imaging Study. J. Neurosci. 19, 3962–3972.

Hoppenbrouwers, S.S., et al., 2008. The role of the cerebellum in the pathophysiology and treatment of neuropsychiatric disorders: a review. Brain Res. Rev. 59, 185–200.

Hu, X., et al., 2019. Localized connectivity in obsessive-compulsive disorder: an investigation combining univariate and multivariate pattern analyses. Cereb. Cortex 13, 122.

Hwang, K., Hallquist, M.N., Luna, B., 2013. The development of hub architecture in the human functional brain network. Cereb. Cortex 23, 2380–2393.

Ito, M., 2008. Control of mental activities by internal models in the cerebellum. Nat. Rev. Neurosci. 9, 304–313.

Josef, P., 2001. Pathological laughter and crying : a link to the cerebellum. Brain. 124, 1708.

Kahnt, T., et al., 2012. Connectivity-based parcellation of the human orbitofrontal cortex. J. Neurosci. 32, 6240–6250.

Kahnt, T., Tobler, P.N., 2017. Dopamine Modulates the Functional Organization of the Orbitofrontal Cortex. J. Neurosci. 37, 1493–1504.

Kellermann, T.S., et al., 2013. Task- and resting-state functional connectivity of brain regions related to affection and susceptible to concurrent cognitive demand. 72, 69-82.

Krienen, F.M., Buckner, R.L., 2009. Segregated fronto-cerebellar circuits revealed by intrinsic functional connectivity. Cereb. Cortex 19, 2485–2497.

Liang, X., et al., 2013. Coupling of functional connectivity and regional cerebral blood flow reveals a physiological basis for network hubs of the human brain. Proc. Natl. Acad. Sci. U. S. A. 110, 1929–1934.

Liu, W., et al., 2020. Disrupted pathways from frontal-parietal cortex to basal ganglia and cerebellum in patients with unmedicated obsessive compulsive disorder as observed by whole-brain resting-state effective connectivity analysis - a small sample pilot study. Brain Imaging Behav.

Luo, Z., et al., 2019. Functional Parcellation of Human Brain Precuneus Using Density-Based Clustering. 1.

Luo, Z., et al., 2020. Functional parcellation of human brain precuneus using density-based clustering. Cereb. Cortex 30, 269–282.

Margulies, D.S., et al., 2009. Precuneus shares intrinsic functional architecture in humans and monkeys. Proc. Natl. Acad. Sci. USA 106, 20069–20074.

Miquel, M., et al., 2019. A working hypothesis for the role of the cerebellum in impulsivity and compulsivity. Front. Behav Neurosci. 13.

Moody, T.D., et al., 2017. Mechanisms of cognitive-behavioral therapy for obsessive-compulsive disorder involve robust and extensive increases in brain network connectivity. Transl. Psychiatr. 7, e1230.

Newman, M.E.J., Girvan, M., 2004. Finding and evaluating community structure in networks. Phys. Rev. E: Stat. Nonlinear Soft Matter Phys. 69, 026113.

O'Reilly, J.X., et al., 2010. Distinct and overlapping functional zones in the cerebellum defined by resting state functional connectivity. Cereb. Cortex 20, 953–965.

Ochsner, K.N., et al., 2004. Reflecting upon feelings: An fMRI study of neural systems supporting the attribution of emotion to self and other. J. Cogn. Neurosci. 16, 1746–1772.

Park, S.E., Jeong, G.W., 2015. Cerebral white matter volume changes in patients with obsessive-compulsive disorder: Voxel-based morphometry. Psychiatry Clin. Neurosci. 69, 717–723.

Pfefferbaum, A., et al., 2011. Cerebral blood flow in posterior cortical nodes of the default mode network decreases with task engagement but remains higher than in most brain regions. Cereb. Cortex 21, 233–244.

Power, J.D., et al., 2012. Spurious but systematic correlations in functional connectivity MRI networks arise from subject motion. Neuroimage. 59, 2142–2154.

Puxeddu, M.G., et al., 2017. Community detection: Comparison among clustering algorithms and application to EEG-based brain networks. Int. Conf. IEEE Eng. Med. Biol. Soc. 3965–3968.

Ramnani, N., 2006. The primate cortico-cerebellar system: anatomy and function. Nat. Rev. Neurosci. 7, 511–522.

Rasgon, A., et al., 2017. Neural correlates of affective and non-affective cognition in obsessive compulsive disorder: A meta-analysis of functional imaging studies. Eur. Psychiat. 46, 25–32.

Ray, S., Turi, R.H., 1999. Determination of number of clusters in K-means clustering and application in colour image segmentation. International Conference on Advances in Pattern Recognition & Digital Techniques.

Robbins, T.W., Vaghi, M.M., Banca, P., 2019. Obsessive-compulsive disorder: puzzles and prospects. Neuron 102, 27–47.

Rosvall, M., Bergstrom, C.T., 2008. Maps of random walks on complex networks reveal community structure. Proc. Natl. Acad. Sci. USA 105, 1118–1123.

Rotge, J.-Y., Guehl, D., 2008. Provocation of obsessive–compulsive symptoms: a quantitative voxel-based meta-analysis of functional neuroimaging studies. J. Psychiatry Neurosci. 33, 405.

Rus, O.G., et al., 2017. Structural alterations in patients with obsessive-compulsive disorder: a surface-based analysis of cortical volume, surface area and thickness. J. Psychiatry Neurosci. 42, 395–403.

Schmahmann, J., 1998. The cerebellar cognitive affective syndrome. Brain. 121, 561–579.

Schmahmann, J.D., 2004. Disorders of the Cerebellum: Ataxia, Dysmetria of Thought, and the Cerebellar Cognitive Affective Syndrome. J. Neurophysiol. 16, 367–378.

Shaw, P., et al., 2015. Subcortical and cortical morphological anomalies as an endophenotype in obsessive-compulsive disorder. Mol. Psychiatr. 20, 224–231.

Stoodley, C.J., Schmahmann, J.D., 2009. Functional topography in the human cerebellum: a meta-analysis of neuroimaging studies. Neuroimage. 44, 489–501.

Tang, W., et al., 2015. Structural brain abnormalities correlate with clinical features in patients with drug-naive OCD: A DARTEL-enhanced voxel-based morphometry study. Behav. Brain Res. 294, 72–80.

Thorsen, A.L., et al., 2018. Emotional processing in obsessive-compulsive disorder: A systematic review and meta-analysis of 25 functional neuroimaging studies. Biol. Psychiat.-Cogn. Neurosci. Neuroimag. 3, 563–571.

Tian, L., et al., 2016. Abnormal functional connectivity of brain network hubs associated with symptom severity in treatment-naive patients with obsessive-compulsive disorder: A resting-state functional MRI study. Prog. Neuro-Psychopharmacol. Biol. Psychiatry 66, 104–111.

Tou, J.T., González, R.C., 1974. Pattern Recognition Principles. Addison-Wesley, Massachusetts.

Tzourio-Mazoyer, N., et al., 2002. Automated anatomical labeling of activations in SPM using a macroscopic anatomical parcellation of the MNI MRI single-subject brain. Neuroimage. 15, 273–289.

van den Heuvel, M.P., Sporns, O., 2011. Rich-club organization of the human connectome. J. Neurosci. 31, 15775–15786.

Viard, A., et al., 2005. Cognitive control in childhood-onset obsessive-compulsive disorder: a functional MRI study. Psychol. Med. 35, 1007–1017.

Viol, K., et al., 2019. Individual OCD-provoking stimuli activate disorder-related and self-related neuronal networks in fMRI. Psychiatry Res. Neuroimaging. 283, 135–144.

von Economo, C.F., Koskinas, G.N., 1925. Die cytoarchitektonik der hirnrinde des erwachsenenmenschen. Springer, Berlin.

Wang, J., et al., 2019. Corresponding anatomical and coactivation architecture of the human precuneus showing similar connectivity patterns with macaques. Neuroimage. 200, 562–574.

Wenderoth, N., et al., 2005. The role of anterior cingulate cortex and precuneus in the coordination of motor behavior. Eur. J. Neurosci. 22, 235–246.

Wu, T., et al., 2013. Cerebellum and integration of neural networks in dual-task processing. Neuroimage. 65, 466–475.

Xu, T., et al., 2019. Altered resting-state cerebellar-cerebral functional connectivity in obsessive-compulsive disorder. Psychol. Med. 49, 1156–1165.

Yun, J.Y., et al., 2020. Brain structural covariance networks in obsessive-compulsive disorder: a graph analysis from the ENIGMA Consortium. Brain. 143, 684–700.

Zhang, S., Li, C.R., 2010. A neural measure of behavioral engagement: Task-residual low-frequency blood oxygenation level-dependent activity in the precuneus. Neuroimage 49, 1911–1918.

Zhang, S., Li, C.R., 2012. Functional connectivity mapping of the human precuneus by resting state fMRI. Neuroimage. 59, 3548–3562.

Zhang, T., et al., 2011. Abnormal small-world architecture of top-down control networks in obsessive-compulsive disorder. J. Psychiatry Neurosci. 36, 23–31.

Zilles, K., Eickhoff, S., Palomero-Gallagher, 2003. The human parietal cortex: a novel approach to its architectonic mapping. Adv. Neurol. 93, 1–21.